The *Tomato brown rugose fruit virus* movement protein overcomes *Tm-2^2* resistance while attenuating viral transport

Hagit Hak and Ziv Spiegelman*

Affiliation:

Department of Plant Pathology and Weed Research, Agricultural Research Organization - the Volcani Center, 68 HaMaccabim Road, P.O.B 15159, Rishon LeZion 7505101, Israel.

*Correspondence: Ziv Spiegelman (ziv.spi@volcani.agri.gov.il).

Abstract

Tomato brown rugose fruit virus (ToBRFV) is a new virus of the *Tobamovirus* genus, causing substantial damage to tomato crops in the Middle East. Reports of recent ToBRFV outbreaks from around the world indicate an emerging global epidemic. ToBRFV overcomes all tobamovirus resistances in tomato, including the durable *Tm-2*^{2} resistance gene. Here, we show that the ToBRFV MP (MP^{ToBRFV}) is the cause for overcoming *Tm-2*^{2} resistance. Transient expression of MP^{ToBRFV} failed to activate the *Tm-2*^{2} resistance response. Replacement of the original MP sequences of *Tomato mosaic virus* (ToMV) with MP^{ToBRFV} enabled this recombinant virus to overcome *Tm-2*^{2} resistance. Hybrid protein analysis revealed that the resistance-breaking elements are located between MP^{ToBRFV} amino acids 1 and 216, and not the C terminus as previously assumed. Interestingly, replacement of *Tobacco mosaic virus* (TMV) and ToMV MPs with MP^{ToBRFV} caused an attenuation of systemic infection of both viruses. Cell-to-cell movement analysis revealed that MP^{ToBRFV} moves less effectively compared to the TMV MP (MP^{TMV}). These findings suggest that overcoming *Tm-2*^{2} is associated with attenuated MP function. This viral fitness cost may explain the high durability of *Tm-2*^{2} resistance, which had remained unbroken for over 60 years.

1. Introduction

The *Tobamovirus* genus is one of the most devastating groups of plant viruses, which includes the *Tobacco mosaic virus* (TMV), *Tomato mosaic virus* (ToMV) and *Cucumber green mottle mosaic virus* (Broadbent, 1976; Rybicki, 2015; Dombrovsky *et al.*, 2017). Tobamoviruses form rod-shaped virions, which encompass a single-stranded, sense RNA genome of about 6.4 kb. This genome encodes four main open reading frames (ORFs): Two subunits of a 126-kDa protein and its read-through 183 kDa variant forming the viral replication complex, a 30-kDa movement protein (MP) and a 17.5 kDa coat protein (CP) (Goelet *et al.*, 1982; Ishibashi and Ishikawa, 2016). Cell-to-cell movement of the virus depends on the viral-encoded MP, which binds to multiple cellular components to transport the viral RNA through plasmodesmata, membrane-lined channels interconnecting adjacent cells (Lucas, 2006; Ueki and Citovsky, 2011; Pitzalis and Heinlein, 2018; Reagan and Burch-Smith, 2020).

A recent outbreak of a new tobamovirus named *Tomato brown rugose fruit virus* (ToBRFV) has substantially damaged the tomato industry in Israel and Jordan, leading to extensive reductions in both yield and fruit quality (Salem *et al.*, 2016; Luria *et al.*, 2017). Recent reports of ToBRFV outbreaks around the world indicate an emerging global epidemic (Cambrón-Crisantos *et al.*, 2018; Yan *et al.*, 2019; Menzel *et al.*, 2019; Ling *et al.*, 2019; Skelton *et al.*, 2019; Fidan *et al.*, 2019; Panno *et al.*, 2019). ToBRFV overcomes all known tobamovirus resistances in tomato, including the durable *Tm-2*^{2} resistance (*R*) gene, and therefore poses a substantial threat for the global tomato industry (Luria *et al.*, 2017).

Dominant resistance (*R*) genes are currently the most powerful means to control plant pathogens (de Ronde *et al.*, 2014). Most of them encode nucleotide-binding leucine-rich repeat (NLR) class of intracellular immune receptors (DeYoung and Innes, 2006). NLRs recognize specific pathogen-encoded effectors either directly or indirectly (Padmanabhan and Dinesh-Kumar, 2014) and trigger an immune signaling cascade that confines the pathogen to the infection site, typically through one of two processes: induction of programmed cell death (PCD) in a process termed hypersensitive response (HR) or extreme resistance, in which resistance is achieved apparently without cell death. Most plant NLRs contain a coiled-coil (CC) or Toll-interleukin-1-receptor (TIR)

homology domain at their N-terminus, a centrally located nucleotide binding (NB) domain, and a leucine rich repeat (LRR) domain at the C-terminus (Burdett *et al.*, 2019).

Resistance against tobamoviruses in tomato was achieved by the introgression of the *R* genes *Tm-1*, *Tm-2* and its allele *Tm-2*^{2} from wild tomato species (Meshi *et al.*, 1989; Ishibashi *et al.*, 2007; Lanfermeijer*et al.*, 2003). In recent decades, resistance-breaking strains have emerged for *Tm-1* and *Tm-2*, leaving *Tm-2*^{2} as the key gene for control of tobamovirus in tomato for the last 60 years (Meshi *et al.*, 1989; Strasser and Pfitzner, 2007). *Tm-2*^{2} encodes a CC-NLR, which associates with its effector, tobamovirus MP, on the plasma membrane to activate an immune response (Weber *et al.*, 1993; Chen *et al.*, 2017). This association confers plant resistance through the induction of either HR or extreme resistance (Hall, 1980), an outcome which depends on the specific level of *Tm-2*^{2} expression (Zhang *et al.*, 2013). Recently it was shown that, upon activation by the MP, Tm-2^2 proteins self-associate on the plasma membrane to form an oligomer that relays the immune signal in a process that depends on both its CC and NB domains (Wang *et al.*, 2020). Previous studies concluded that the C-terminal part of MP is essential for recognition by Tm-2^2 (Weber *et al.*, 1993; Weber and Pfitzner, 1998); two amino-acid substitutions at the ToMV MP (MP^{ToMV}) C terminus of the resistance-breaking ToMV isolate ToMV-2^2, S238R and K244E, were found to overcome *Tm-2*^{2} resistance (Weber *et al.*, 1993). Moreover, a premature stop codon in MP^{ToMV}, causing truncation of the MP C-terminal 30 amino acids, enabled ToMV to overcome *Tm-2*^{2} resistance (Weber and Pfitzner, 1998).

ToBRFV is currently the only known tobamovirus that overcomes *Tm-2*^{2} resistance (Luria *et al.*, 2017). Previous sequence analysis showed that ToBRFV contains 21 potential resistance-breaking mutations. Of those, 12 mutations are located in the ToBRFV MP (MP^{ToBRFV}) and likely contribute to overcoming *Tm-2*^{2} (Maayan *et al.*, 2018). These include mutations that potentially change protein features such as secondary structures, phosphorylation sites and disulfide bonds. However, so far, there was no experimental evidence for the role of MP^{ToBRFV} in overcoming *Tm-2*^{2} resistance.

Here, we show that MP^{ToBRFV} overcomes *Tm-2*^{2} resistance, independent of its C-terminal part. In addition, we show that overcoming *Tm-2*^{2} is associated with reduced systemic and cell-to-cell movement, suggesting that the resistance-breaking elements

have negative effects on MP^{ToBRFV} function. These findings may explain the high durability of *Tm-2*^{2}, which has only been broken recently by ToBRFV.

2. Results

2.1 MP^{ToBRFV} does not trigger *Tm-2*^{2}-mediated cell death

Activation of NLR receptors by their effectors can be monitored by the appearance of HR-mediated cell death when the NLR is co-expressed with its effector (Whitham *et al.* 1996; Moffett *et al.*, 2002; Wu *et al.*, 2015). Multiple studies showed that co-expression of MP^{TMV} and *Tm-2*^{2} can trigger HR in *N. benthamiana* (Zhang *et al.*, 2013; Chen *et al.*, 2017; Wang *et al.*, 2020). To test if Tm-2^2 recognizes MP^{ToBRFV}, the coding sequences of MP^{ToBRFV} and MP^{TMV} were cloned under the control of the *35S* promoter (*p35S:*MP^{ToBRFV} and *p35S:*MP^{TMV}, respectively). Clones were then transiently expressed in leaflets of tomato cv. Ikram (a *Tm-2*^{2}*/tm-2* heterozygote) using agroinfiltration (Figure 1 a-c). When *p35S:*MP^{TMV} was expressed, cell death was observed in infiltrated leaflets as a result of immune response activation (Figure 1a). On the other hand, leaflets infiltrated with *p35S:*MP^{ToBRFV} showed only marginal necrosis (Figure 1b), similar to that of the empty vector control treatment (Figure 1c). To confirm that these findings are a direct result of *Tm-2*^{2} activity, a similar experiment was performed with *N. benthamiana*. Here again, transient co-expression of *p35S:*MP^{TMV} with *p35S:Tm-2*^{2} caused marked lesions and electrolyte leakage consistent with the establishment of HR (Figure 1d and i), while co-expression of *p35S:*MP^{ToBRFV} with *p35S:Tm-2*^{2} resulted in minimal cell death (Figure 1e) and reduced electrolyte leakage (Figure 1i). Individual expression of *Tm-2*^{2}, MP^{ToBRFV} and MP^{TMV} resulted in no cell death or electrolyte leakage (Figure 1f-i). The marginal immune activation by MP^{ToBRFV} indicated that this protein was able to evade *Tm-2*^{2} resistance.

2.2 A recombinant clone of ToMV harboring MP^{ToBRFV} overcomes *Tm-2*^{2} resistance in tomato

To test the ability of MP^{ToBRFV} to overcome *Tm-2*^{2} resistance in tomato, a hybrid clone was generated based on an existing infectious clone of ToMV (Hamamoto *et al.*, 1993). The original MP sequence of ToMV was replaced with MP^{ToBRFV} ($ToMV^{MP\text{-}ToBRFV}$) (Figure 2a). This clone was then used to infect tomato plants homozygous for

the ToMV-sensitive *tm-2* allele or the *Tm-2*^{2} allele (Figure 2b). Viral RNA was quantified in infected and systemic leaves (Figure 2c and d, respectively) using RT-qPCR. As expected, inoculation of *tm-2* plants with ToMV resulted in severe viral symptoms (Figure 2b) and high level of viral accumulation in both infected and systemic leaves (Figure 2c-e), while *Tm-2*^{2} plants were completely immune to ToMV (Figure 2b-e). In marked contrast, ToMV$^{MP\text{-}ToBRFV}$ induced symptoms in both *tm-2* and *Tm-2*^{2} plants (Figure 2b and e) and viral accumulation was detected in plants harboring both alleles (Figure 2c-e). It is important to note that in both *tm-2* and *Tm-2*^{2} ToMV$^{MP\text{-}ToBRFV}$ symptoms were milder than those of ToMV-infected *tm-2* plants (Figure 2b), suggesting that MP^{ToBRFV} reduced ToMV pathogenicity. Together, these results established that MP^{ToBRFV} is sufficient to overcome *Tm-2*^{2} resistance.

2.3 The MP^{ToBRFV} C terminus is dispensable for overcoming Tm-2^2

To characterize the potential resistance-breaking elements in MP^{ToBRFV}, a protein sequence alignment was performed on MP^{ToBRFV}, MP^{TMV}, MP^{ToMV} and the MP of the *Tm-2*^{2} resistance-breaking ToMV isolate ToMV-2^2 (MP$^{ToMV\text{-}2^2}$) (Figure 3a). At the whole protein level, MP^{ToBRFV} was 81% identical to MP^{ToMV} and 78% identical MP^{TMV}. However, at the C-terminal 50 amino acids (216-266) (Figure 3a, broken line), the sequence was more variable (41% and 42% identity with MP^{ToMV} and MP^{TMV}, respectively). Importantly, this region includes the C-terminal 30 amino acids and MP^{ToMV} amino acids S238 and K244, previously shown to be essential for recognition by *Tm-2*^{2} (Figure 3a, yellow) (Weber and Pfitzner, 1993; Weber *et al.*, 1998). This suggested that the MP^{ToBRFV} C terminus is the resistance-breaking factor.

To test if the MP^{ToBRFV} C terminus overcomes *Tm-2*^{2}, two hybrid MP clones were generated (Figure 3b): the first containing MP^{TMV} amino acids 1-216 fused the MP^{ToBRFV} C-terminal 50 amino acids 217-266 (MP$^{TMV\ 1\text{-}216}$/MP$^{ToBRFV\ 217\text{-}266}$) and the second containing MP^{ToBRFV} amino acids 1-216 fused to MP^{TMV} amino acids 217-266 (MP$^{ToBRFV\ 1\text{-}216}$/MP$^{TMV\ 217\text{-}266}$) (Figure 3b). Co-expression of *p35s:Tm-2*^{2} with MP$^{TMV\ 1\text{-}216}$/MP$^{ToBRFV\ 217\text{-}266}$ induced strong HR, indicating that the MP^{ToBRFV} C terminus was insufficient to evade *Tm-2*^{2} (Figure 3b and c). In addition, the MP$^{ToBRFV\ 1\text{-}216}$/MP$^{TMV\ 217\text{-}266}$ fusion did not trigger cell death when co-expressed with *Tm-2*^{2} (Figure 3b and c). To verify that the MP^{TMV} C-terminal region is not required for *Tm-2*^{2} recognition, a

clone with a truncated version of MP^{TMV} containing a stop codon in position 238 was generated ($MP^{TMV\ \Delta 30}$). Here again, a marked HR was observed when $MP^{TMV\ \Delta 30}$ was co-expressed with *Tm-2*^{2}, suggesting that the MP^{TMV} C-terminus is dispensable for *Tm-2*^{2} recognition (Figure 3b and c).

To confirm these results in tomato, a hybrid ToMV clone was generated with MP^{ToBRFV} amino acids 1-216 fused to MP^{ToMV} amino acids 217-266 (Figure 3d). Viral transcripts were detected in infected and systemic leaves of both *tm-2* and *Tm-2*^{2} plants 3 weeks after inoculation (Figure 3e and f), establishing that this virus was able to overcome *Tm-2*^{2} resistance, regardless of the MP^{ToBRFV} C terminus.

2.4 MP^{ToBRFV} attenuates systemic viral infection of TMV-GFP and ToMV

Overcoming dominant resistance is often associated with viral fitness costs (García-Arenal and Fraile, 2013). Since MP^{ToBRFV}, which overcomes *Tm-2*^{2} resistance, also caused reduced symptoms in *tm-2* tomato plants (Figure 3b), we hypothesized that the function of MP^{ToBRFV} is reduced as compared to other MPs. To test this, a TMV-GFP clone (Lindbow, 2007) harboring MP^{ToBRFV} instead of its original MP (TMV-$GFP^{MP\text{-}ToBRFV}$) was generated. Local and systemic infection were determined 7 days after inoculation (dpi) of *N. benthamiana* plants using GFP *in vivo* imaging analysis (IVIS) (Figure 4). While TMV-GFP showed strong fluorescence in both locally infected and systemic leaves (Figure 4a, d-f), the resistance-breaking TMV-$GFP^{MP\text{-}ToBRFV}$ hybrid showed weaker fluorescent signals (Figure 4b, d-f). To confirm that the reduced infection was due to the attenuated function of MP^{ToBRFV}, a rescue assay was done by co-agroinfiltrating TMV-$GFP^{MP\text{-}ToBRFV}$ with *p35S:MP*^{TMV}. Interestingly, MP^{TMV} partially rescued the effect of MP^{ToBRFV} on systemic spread of the virus (Figure 4c and d), leading to a 2-fold increase in local infection and a 4-fold increase in systemic accumulation of the virus (Figure 4e and f, respectively). These results suggested that MP^{ToBRFV} is less effective than MP^{TMV} in promoting viral spread, likely due to its reduced function in cell-to-cell transport of the virus.

We further monitored the effect of MP^{ToBRFV} on systemic spread in *tm-2* tomato plants by western blot analysis of CP accumulation (Figure 5). Time course analysis of virus accumulation was performed in systemic tomato leaves 4, 8 and 12 dpi of plants infected with ToMV, $ToMV^{MP\text{-}ToBRFV}$ and ToBRFV (Figure 5a). ToMV was first detected in systemic leaves at 4 dpi, while the viruses harboring MP^{ToBRFV}, $ToMV^{MP\text{-}}$

^{ToBRFV} and ToBRFV, were barely detected. At 8 dpi, ToBRFV and ToMV$^{MP\text{-}ToBRFV}$ could be detected in systemic leaves, however, their signal was significantly weaker than ToMV (Figure 5a and b). At 12 dpi there was no significant differences in accumulation of all three viruses. These results suggest that, while MP^{ToBRFV} confers the ability to overcome *Tm-2*^{2}, it also reduces the rate of systemic infection compared to MP^{TMV} and MP^{ToMV}.

2.5 Reduced cell-to-cell transport of MP^{ToBRFV} compared to MP^{TMV}

Since the role of a MP is to enable intercellular transport of the viral RNA, we speculated that the reduction of systemic infection caused by MP^{ToBRFV} is a result of a decrease in cell-to-cell movement. To monitor cell-to-cell movement, the ORFs of both *MP*^{TMV} and *MP*^{ToBRFV} were fused to *YFP* and expressed under the *35S* promoter (Figure 6a and d) in *N. benthamiana* leaves. As an immobile control, ER-targeted mCherry (ER-mCherry) was expressed from the same binary plasmid, to mark the original cell of expression (Figure 6b and e). Low dilution (OD = 0.0001) of agrobacterium was used to express the constructs in individual *N. benthamiana* epidermal cells and z-stack confocal images were taken for each cell. The result was cell clusters, in which the central cell expressed the MP and the proximal cells contained the trafficked MP (Figure 6c and f). The number of adjacent cells containing the trafficked MP^{TMV}-YFP and MP^{ToBRFV}-YFP was used to quantify the level of intercellular movement. Interestingly, while MP^{TMV}-YFP moved to an average of 9.28±0.38 cells (n = 64), MP^{ToBRFV}-YFP moved to an average of 6.8±0.38 cells (n = 51) (Figure 6g). In addition, movement to ≥10 cells was evident in 48.4% of MP^{TMV}-YFP cell clusters, but only in 13.2% of MP^{ToBRFV}-YFP cell clusters. Consistently, movement to ≤4 cells was detected in 25.5% of MP^{ToBRFV}-YFP but only 6.25% of MP^{TMV}-YFP (Figure 6h). These results show that MP^{ToBRFV} intercellular movement is reduced as compared to MP^{TMV}.

3. Discussion

ToBRFV is a significant threat to tomato production worldwide. This highly infectious virus can be easily transmitted by seed coats, working hands, tools, soil and beneficial pollinators (Smith and Dombrovsky, 2019; Levitzky *et al.*, 2019; Klap *et al.*, 2020a). In addition, interaction of ToBRFV with other viruses may increase their disease severity (Luria *et al.*, 2018; Klap *et al.*, 2020b). The main cause for the global ToBRFV

outbreak is that this novel virus overcame the long-standing *Tm-2^2* resistance. Since *Tm-2^2*-based resistance remained unbroken for decades, the question of which factors caused this resistance to break is of agricultural and scientific importance. Previous studies established that the viral MP is recognized by Tm-2^2 to trigger resistance against the virus. Therefore, in the current study, we investigated the role of MP^{ToBRFV} in overcoming *Tm-2^2*. Our findings establish that *Tm-2^2* is not activated by MP^{ToBRFV} (Figure 1), and that MP^{ToBRFV} is sufficient to overcome *Tm-2^2* (Figure 2). These findings are consistent with previous findings on the role of the viral MP as the target of Tm-2^2 resistance and establish MP^{ToBRFV} as the *Tm-2^2* resistance-breaking factor (Meshi *et al.*, 1989; Weber *et al.*, 1993).

While it has been shown that the C-terminal part of MP is essential for recognition by Tm-2^2 (Weber *et al.*, 1993; Weber and Pfitzner, 1998), later studies suggested that the C-terminal part of the MP is dispensable for recognition by Tm-2^2. Expression of a truncated version of MP^{ToMV}, consisting of only the N-terminal 188 amino acids, was sufficient to trigger the *Tm-2^2* immune response, while expression of the C-terminal 76 amino acids alone did not activate *Tm-2^2* resistance (Weber *et al.*, 2004). In addition, a TMV MP (MP^{TMV}) variant with a C-terminal 81 amino acid deletion still activated *Tm-2^2* resistance in *N. benthamiana* (Chen *et al.*, 2017). Here, we showed that the MP^{ToBRFV} C-terminal part does not determine *Tm-2^2* recognition or avoidance. Instead, it seemed that elements within MP^{ToBRFV} amino acids 1-216 overcome this resistance. Computational analysis of MP^{ToBRFV} revealed 12 potential resistance-breaking amino acids, which are not conserved with MP^{TMV} and MP^{ToMV} and can alter the protein charge, structure or phosphorylation, many of which are located between amino acids 1 and 216 (Maayan *et al.*, 2018). Our study provides a platform for elucidating the precise MP^{ToBRFV} amino acids are required to overcome *Tm-2^2*.

Overcoming host resistance is often associated with reductions in viral fitness (García-Arenal and Fraile, 2013). There are numerous examples in which resistance-breaking mutations cause penalties in viral infectivity or competition. For example, resistance-breaking mutations in the *Potato virus Y* Nla protein, which overcome the *R* gene *Ry*, also caused loss of its protease activity (Mestre *et al.*, 2003). Mutations in *Turnip mosaic virus* which overcome TuRB01 and TuRB04 resistances in *Brassica napus* impaired the virus's ability to compete with a non-resistance-breaking viral strain on a susceptible host (Jenner *et al.*, 2002). ToMV replicase mutations that overcome

Tm-1 resistance also cause an attenuation of viral replication (Ishibashi *et al.*, 2012). Recently, it was shown that resistance-breaking mutations in the *Pepper mild mottle virus* coat protein variously affect viral particle stability (Bera *et al.*, 2019). Here, we show that overcoming *Tm-2*^{2} resistance by MP^{ToBRFV} is associated with delayed viral spread and cell-to-cell movement (Figures 4 to 6).

Previous reports suggested that overcoming *Tm-2*^{2} might require mutations that impair viral movement or survival, and that existing *Tm-2*^{2} resistance-breaking isolates display reduced transmissibility (Hall, 1980). Indeed, MP^{ToBRFV} amino acids 1-216 include elements essential for MP function (Maayan et al., 2018), including plasmodesmal localization signal (Yuan *et al.*, 2016), a region essential for increasing plasmodesmal size exclusion limit (Weigmann *et al.*, 1994), endoplasmic reticulum interaction domain (Peiró *et al.*, 2014) and RNA binding domains (Citovsky *et al.*, 1992). In addition, the MP C-terminal 50 amino acids, which are dispensable for overcoming *Tm-2*^{2} (Figure 3), are also non-essential for viral movement (Berna *et al.*, 1991). The finding that MP^{ToBRFV} activity is reduced compared to MP$^{TMV/ToMV}$ supports the hypothesis that *Tm-2*^{2} targets MP sequences essential for its function.

In light of these findings, one may wonder how ToBRFV was able to break this resistance, whereas TMV and ToMV failed to do so. To address this question, we propose the hypothetical model outlined in Figure 7. According to this model, resistance-breaking mutations are required for MP^{ToMV} or MP^{TMV} to overcome Tm-2^2 (Figure 7a). These resistance-breaking mutations would likely impair MP function leading to loss of viral movement, and eventually loss of infectivity or pathogenicity (Figure 7b). Reconstitution of viral movement would require additional compensatory mutations for MP to retain functionality (Figure 7c). The requirement of multiple mutations to overcome *Tm-2*^{2} combined with high levels of fitness penalties would be highly unlikely or rare and uncompetitive. ToBRFV, on the other hand, likely evolved on an unknown host (Maayan *et al.*, 2018), and invaded tomato due to a host shifting event (Figure 7d). Evolution on another host allowed MP^{ToBRFV} to diverge from MP^{TMV} and MP^{ToMV}, in a manner that will allow it to evade *Tm-2*^{2}, yet sustain sufficient levels of movement (Figure 7d).

Collectively, our results establish MP^{ToBRFV} as the *Tm-2*^{2} resistance-breaking factor. Based on our systemic and cell-to-cell movement assays, we propose that the

mutations that prevented activation of Tm-2^2 may have also affected MP function. This may explain the high durability of *Tm-2^2* against TMV and ToMV. We conclude that the MP^{ToBRFV} protein sequence balances between *Tm-2^2* evasion and viral movement.

4. Experimental procedures

4.1 Plant materials

Tomato *(Solanum lycopersicum* L.) seeds (cv. Moneymaker) homozygous for the *tm-2* allele (LA2706) or the *Tm-2^2* allele (LA3310) were obtained from the Tomato Genome Research Center (TGRC), University of California, Davis. Tomato plants cv. Ikram were obtained from Syngenta Co. *Nicotiana benthamiana* and tomato plants were grown in soil in a light- and temperature-controlled chamber at 25°C with a 16h light/8h dark regime. Five-week- old *N. benthamiana* plants were used for agroinfiltration of TMV-GFP and three-week-old tomato plants were used for mechanical inoculation of ToMV.

4.2 Plasmid Construction

The various MP^{TMV}/MP^{ToBRFV} hybrids were generated using fusion PCR. The following binary plasmids were assembled by Golden Gate cloning using the MoClo Tool Kit for plants (Addgene kit #1000000044) (Weber *et al.*, 2011). *p35S:Tm-2^2*, *p35S:MP^{TMV}* and *p35S:MP^{ToBRFV}* were generated by cloning the *Tm-2^2* (AF536201), MP^{TMV} and MP^{ToBRFV} ORFs into pICH486988, a binary Level 2 Golden Gate vector that contains an expression cassette under the CaMV *35S* promoter. To allow Golden Gate assembly, internal BsaI sites were removed by one-step cloning. Plasmids containing the double expression cassettes *p35S:MP^{TMV}-YFP; ER-mCherry* and *p35S:MP^{ToBRFV}-YFP; ER-mCherry* were assembled using the Level 2 vector pAGM4673. The ER-mCherry sequence were amplified from the *ER-rk CD3-959* plasmid (Nelson *et al.*, 2007), containing the mCherry ORF with the *Arabidopsis thaliana wall-associated kinase 2* signal peptide at the N-terminus of the ER His-Asp-Glu-Leu retention signal at its C-terminus.

pTLW3 is a cDNA vector harboring the full ToMV sequence under the T7 promoter (Hamamoto *et al.*, 1993). $ToMV^{MP\text{-}ToBRFV}$ was assembled by fusion PCR and the MP^{ToBRFV} ORF was inserted between the KpnI and XmaI sites of the vector.

The binary vector pJL24 (Lindbow, 2007) contains the full TMV genome with the GFP gene upstream to the MP ORF, and is named here TMV-GFP. The MP^{ToBRFV} ORF was amplified from RNA extracted from ToBRFV-infected plants (accession no. KX619418.1) and was cloned between the AgeI and PacI sites of the pJL24 vector using fusion PCR to create TMV-$GFP^{MP\text{-}ToBRFV}$.

4.3 Transient expression and agro-infiltration

Agrobacterium tumefaciens strain EHA105 harboring a binary vector were grown overnight at 28°C. Cell cultures were resuspended in MES buffer (10mM MgCl2, 10mM MES, 150µM acetosyringone, pH 5.6) to an optical density of OD_{600} = 0.5 (or OD600 = 0.0001 for cell-to-cell movement experiments) and infiltrated using a needleless syringe into the abaxial side of the 4th or 5th leaf of *N. benthamiana.*

4.4 Electrolyte leakage assay

p35S:Tm-2[2] and *p35S:MP* constructs were agroinfiltrated at OD_{600}=0.25 individually or at a 1:1 ratio as indicated to *N. benthamiana* leaves. Twenty-seven hours later, four leaf discs (1 cm diameter) were cut out of each leaf and washed for 10-30 minutes in distilled water. The leaf discs were then carefully transferred into a tube containing 4 ml of distilled water and placed in a growth chamber. Electric conductivity was measured after 6 hours using a benchtop conductivity meter.

4.5 TMV-GFP infection and quantification

A. tumefaciens harboring TMV-GFP or TMV-$GFP^{MP\text{-}ToBRFV}$ vectors was infiltrated into the fourth leaf of 4-week-old *N. benthamiana* plants. GFP fluorescence was monitored 6 days post infiltration. Images were acquired and analyzed using In Vivo Imaging System (IVIS Lumina LT, PerkinElmer) equipped with a XFOV-24 lens and Living Image 4.3.1 software (PerkinElmer) set (excitation/emission: 420 nm/520 nm). The optical luminescent image data was displayed in pseudocolor that represents intensity in terms of Radiance (photons/sec/cm^2/steradian) and calculated as average radiance per leaf.

4.6 *In vitro* transcription and infection

2µl of ToMV pTLW3 plasmid, $ToMV^{MP\text{-}ToBRFV}$ or $ToMV^{MP\text{-}ToBRFV(1\text{-}216)}$ were linearized with SmaI and cleaned by Gel extraction kit (Zymo Research, ZR-D4002). *In vitro* transcription using the mMESSAGE mMACHINE™ T7 kit (Invitrogen by Thermo Fisher Scientific, AM1344) was performed according to manufacturer's instructions.

Two drops of 2.5µl of transcript were used to mechanically inoculate *N. benthamiana* plants that were dusted with carborundum powder prior to inoculation. Leaves of the infected plants were collected after 5-7 dpi to serve as inoculum for tomato plants.

4.7 Evaluation of ToMV levels by RT-qPCR Analysis

Total RNA was extracted from 50-100 mg of leaf tissue by Plant Total RNA Mini Kit (Geneaid, RPD050), which includes a DNAse treatement. RNA (500 ng) served as a template for cDNA synthesis (PCRBIO, PB30.11). RT-qPCR was performed using 2xSyGreen Mix (PCRBIO, PB20.16) in a Rotor-Gene 6000 cycler (Corbett Research). ToMV levels were calculated as the expression ratio of ToMV-CP and the gene of reference, TIP41 (Lacerda *et al.*, 2015).

4.8 Evaluation of ToMV and ToBRFV levels by SDS-PAGE and Western blot

For detection of the spread of the virus in tomato, the first small leaf (1-3 cm) and apex were collected and ground while frozen in a microcentrifuge tube. Laemmli buffer (40 µl of 3x) (100 mM Tris, 2% SDS, 20% glycerol, 4% β-mercaptoethanol, pH 6.8) were added and mixed into the sample, followed by 10 min centrifugation and 5 min boiling of the supernatant. Samples were run on 12% SDS-PAGE acrylamide gels, transferred to nitrocellulose membranes (Protran, #10401380) and blocked with 3% skimmed milk in Tris buffer saline (TBS)-Tween. CP of the virus was detected by rabbit anti-Tobamovirus CP; 1:20,000 (courtesy of Dr. Aviv Dombrovsky), and anti-Rabbit HRP; 1:20,000 (Jackson Immunoresearch, #323-005-021.). Chemiluminescence was observed using Elistar Supernova as substrate (Cyanagen, #XLSE2) and images of protein bands were acquired and quantified using the Alliance UVITEC software.

4.9 Cell-to-cell movement analysis

Constructs expressing MP-YFP and ER-mCherry were agroinfiltrated into *N. benthamiana* and visualized 36 hours later. For confocal imaging, we used an Olympus IX 81 inverted laser scanning confocal microscope (Fluoview 500) equipped with an OBIS 488 and 561 nm laser lines and a 60× 1.0 NA PlanApo water immersion objective. YFP and mCherry were excited at 488 and 561 nm and imaged using BA505-525 nm and BA575–620 nm emission filters respectively. The number of YFP-fluorescent cells surrounding the original cell of expression was quantified to determine the level of movement for each MP.

Acknowledgements

We would like to thank Prof. Manfred Heinlein (CNRS, France), Prof. Bryce Falk (UC Davis, USA) for providing the TMV-GFP plasmid and Prof. Masayuki Ishikawa (NARO, Japan) for kindly providing the ToMV infectious clone. We also thank Dr. Aviv Dombrovsky for anti-tobamovirus CP antibody and Prof. Ilan Levin (ARO, Israel) for the tomato (cv. Moneymaker) lines used in the manuscript. We thank Dr. Amit Gal-On (ARO, Israel), Dr. Victor Gaba (ARO, Israel) and Dr. Munir Mawassi (ARO, Israel) for their valuable advice and critical reading of this manuscript. This work was funded by grant number 20-02-0130 from the Chief Scientist, Israeli Ministry of Agriculture.

Conflict of interests

The authors declare no conflict of interests.

Author contributions

HH and ZS designed the research, conducted the experiments and wrote the manuscript.

Data availability statement

The data that support the findings of this study are available from the corresponding author upon reasonable request.

References

Bera, S., Moreno-Pérez, M. G., García-Figuera, S., Pagán, I., Fraile, A., Pacios, L. F. and García-Arenal, F. (2017) Pleiotropic effects of resistance-breaking mutations on particle stability provide insight into life history evolution of a plant RNA virus. *Journal of virology*, **91,** e00435-17.

Berna, A., Gafny, R., Wolf, S., Lucas, W. J., Holt, C. A., and Beachy, R.N. (1991) The TMV movement protein: role of the C-terminal 73 amino acids in subcellular localization and function. *Virology*, **182**, 682-689.

Broadbent, L. (1976) Epidemiology and control of *tomato mosaic virus*. *Annual*

review of Phytopathology, **14**, 75-96.

Burdett, H., Bentham, A. R., Williams, S. J., Dodds, P. N., Anderson, P. A., Banfield, M. J. and Kobe, B. (2019) The plant "Resistosome": Structural insights into immune signaling. *Cell host & microbe*, **26**, 193-201.

Cambrón-Crisantos, J. M., Rodríguez-Mendoza, J., Valencia-Luna, J. B., Rangel, S. A., de Jesús García-Ávila, C., and López-Buenfil, J. A. (2018) First report of *Tomato brown rugose fruit virus* (ToBRFV) in Michoacan, Mexico. *Mexican Journal of Phytopathology*, **37**, 185-192.

de Ronde, D., Butterbach, P., and Kormelink, R. (2014). Dominant resistance against plant viruses. *Frontiers in plant science*, **5**, 307.

Chen, T., Liu, D., Niu, X., Wang, J., Qian, L., Han, L., Liu, N., Zhao, J., Hong, Y., and Liu, Y. (2017) Antiviral resistance protein Tm-2^2 functions on the plasma membrane. *Plant physiology*, **173**, 2399-2410.

Citovsky, V., Wong, M. L., Shaw, A. L., Prasad, B. V., and Zambryski, P. (1992) Visualization and characterization of *tobacco mosaic virus* movement protein binding to single-stranded nucleic acids. *The Plant Cell*, **4**, 397-411.

DeYoung, B. J. and Innes, R. W. (2006) Plant NBS-LRR proteins in pathogen sensing and host defense. *Nature immunology*, **7**, 1243.

Dombrovsky, A., Tran-Nguyen, L. T. and Jones, R. A. (2017) *Cucumber green mottle mosaic virus*: rapidly increasing global distribution, etiology, epidemiology, and management. *Annual review of phytopathology*, **55**, 231-256.

Fidan, H., Sarikaya, P. and Calis, O. (2019) First report of *Tomato brown rugose fruit virus* on tomato in Turkey. *New Disease Reports*, **39**, 2044-0588.

Goelet, P., Lomonossoff, G. P., Butler, P. J., Akam, M. E., Gait, M. J. and Karn, J. (1982) Nucleotide sequence of *Tobacco mosaic virus* RNA. *Proceedings of the National Academy of Sciences*, **79**, 5818-5822.

Hall, T. J. (1980) Resistance at the *Tm-2* locus in the tomato to *tomato mosaic virus*. *Euphytica*, **29**, 189-197.

Hamamoto, H., Sugiyama, Y., Nakagawa, N., Hashida, E., Matsunaga, Y. *et al.* (1993) A new *tobacco mosaic virus* vector and its use for the systemic production of angiotensin-I-converting enzyme inhibitor in transgenic tobacco and tomato. *Bio/technology*, **11**, 930-932.

Ishibashi, K. and Ishikawa, M. (2016) Replication of tobamovirus RNA. *Annual Review of Phytopathology*, **54**, 55-78.

Ishibashi, K., Masuda, K., Naito, S., Meshi, T., and Ishikawa, M. (2007) An inhibitor of viral RNA replication is encoded by a plant resistance gene. *Proceedings of the National Academy of Sciences*, *104*(34), 13833-13838.

Ishibashi, K., Mawatari, N., Miyashita, S., Kishino, H., Meshi, T. and Ishikawa, M. (2012) Coevolution and hierarchical interactions of *Tomato mosaic virus* and the resistance gene *Tm-1*. *PLoS Pathogens*, **8**, e1002975.

Jenner, C. E., Wang, X., Ponz, F. and Walsh, J. A. (2002) A fitness cost for *Turnip mosaic virus* to overcome host resistance. *Virus research*, **86**, 1-6.

Klap, C., Luria, N., Smith, E., Bakelman, E., Belausov *et al.* (2020a) The Potential Risk of Plant-Virus Disease Initiation by Infected Tomatoes. *Plants*, 9, 623.

Klap, C., Luria, N., Smith, E., Hadad, L., Bakelman, E. *et al.* (2020b) Tomato Brown Rugose Fruit Virus Contributes to Enhanced Pepino Mosaic Virus Titers in Tomato Plants. Viruses, **12**, 879.

Lacerda, A. L., Fonseca, L. N., Blawid, R., Boiteux, L. S., Ribeiro, S. G. and Brasileiro, A. C. (2015) Reference gene selection for qPCR analysis in tomato-bipartite begomovirus interaction and validation in additional tomato-virus pathosystems. *PLoS One*, **10**, e0136820.

Lanfermeijer, F. C., Dijkhuis, J., Sturre, M. J., de Haan, P. and Hille, J. (2003) Cloning and characterization of the durable *Tomato mosaic virus* resistance gene $Tm\text{-}2^2$ from *Lycopersicon esculentum*. *Plant molecular biology*, **52**, 1039-1051.

Lanfermeijer, F. C., Warmink, J. and Hille, J. (2005) The products of the broken *Tm-2* and the durable $Tm\text{-}2^2$ resistance genes from tomato differ in four amino acids. *Journal of experimental botany*, **56**, 2925-2933.

Lindbo, J. A. (2007) High-efficiency protein expression in plants from agroinfection-compatible *Tobacco mosaic virus* expression vectors. *BMC biotechnology*, **7**, 52.

Ling, K. S., Tian, T., Gurung, S., Salati, R. and Gilliard, A. (2019) First report of *Tomato brown rugose fruit virus* infecting greenhouse tomato in the United States. *Plant Disease*, **103**, 1439.

Luria, N., Smith, E., Reingold, V., Bekelman, I., Lapidot, M. *et al.* (2017) A new Israeli Tobamovirus isolate infects tomato plants harboring $Tm\text{-}2^2$ resistance genes. *PLoS one*, **12**, e0170429.

Luria, N., Smith, E., Sela, N., Lachman, O., Bekelman, I., Koren, A. and Dombrovsky, A. (2018) A local strain of *Paprika mild mottle virus* breaks *L3* resistance

in peppers and is accelerated in *Tomato brown rugose fruit virus*-infected *Tm-2*^{2}-resistant tomatoes. *Virus genes*, **54**, 280-289.

Maayan, Y., Pandaranayaka, E. P., Srivastava, D. A., Lapidot, M., Levin, I., Dombrovsky, A. and Harel, A. (2018) Using genomic analysis to identify tomato *Tm-2* resistance-breaking mutations and their underlying evolutionary path in a new and emerging tobamovirus. *Archives of virology*, **163**, 1863-1875.

Menzel, W., Knierim, D., Winter, S., Hamacher, J. and Heupel, M. (2019) First report of *Tomato brown rugose fruit virus* infecting tomato in Germany. *New Disease Reports*, **39**, 2044-0588.

Meshi, T., Motoyoshi, F., Maeda, T., Yoshiwoka, S., Watanabe, H. and Okada, Y. (1989) Mutations in the *tobacco mosaic virus* 30-kD protein gene overcome *Tm-2* resistance in tomato. *The Plant Cell*, **1**, 515-522.

Mestre, P., Brigneti, G., Durrant, M. C. and Baulcombe, D. C. (2003) *Potato virus Y* NIa protease activity is not sufficient for elicitation of *Ry*-mediated disease resistance in potato. *The Plant Journal*, **36**, 755-761.

Moffett, P., Farnham, G., Peart, J. and Baulcombe, D. C. (2002) Interaction between domains of a plant NBS–LRR protein in disease resistance-related cell death. *The EMBO journal*, **21**, 4511-4519.

Nelson, B.K., Cai, X. and Nebenführ, A. (2007) A multicolored set of in vivo organelle markers for co-localization studies in *Arabidopsis* and other plants. *The Plant Journal*, **51**, 1126-1136.

Padmanabhan, M.S. and Dinesh-Kumar, S.P. (2014) The conformational and subcellular compartmental dance of plant NLRs during viral recognition and defense signaling. *Current opinion in microbiology*, **20**, 55-61.

Panno, S., Caruso, A.G. and Davino, S. (2019) First report of *tomato brown rugose fruit virus* on tomato crops in Italy. *Plant Disease*, **103**, 1443-1443.

Peiró, A., Martínez-Gil, L., Tamborero, S., Pallás, V., Sánchez-Navarro, J. A. and Mingarro, I. (2014) The *Tobacco mosaic virus* movement protein associates with but does not integrate into biological membranes. *Journal of virology*, **88**, 3016-3026.

Pitzalis, N. and Heinlein, M. (2018) The roles of membranes and associated cytoskeleton in plant virus replication and cell-to-cell movement. *Journal of Experimental Botany*, **69**, 117-132.

Reagan, B.C. and Burch-Smith, T.M. (2020) Viruses reveal the secrets of plasmodesmal cell biology. *Molecular Plant-Microbe Interactions*, **33**, 26-39.

Rybicki, E.P. (2015) A Top Ten list for economically important plant viruses. *Archives of Virology*, **160**, 17-20.

Salem, N., Mansour, A., Ciuffo, M., Falk, B. W. and Turina, M. (2016) A new tobamovirus infecting tomato crops in Jordan. *Archives of Virology*, **161**, 503-506.

Skelton, A., Buxton-Kirk, A., Ward, R., Harju, V., Frew, L. *et al.* (2019) First report of *Tomato brown rugose fruit virus* in tomato in the United Kingdom. *New Disease Reports*, **40**, 12.

Smith, E., and Dombrovsky, A. (2019) Aspects in Tobamovirus Management in Intensive Agriculture. In: S. Topolovec-Pintaric (Ed.) *Plant Diseases-Current Threats and Management Trends*. London, UK: IntechOpen, 10.5772/intechopen.87101.

Strasser, M. and Pfitzner, A.J.P. (2007) The double-resistance-breaking *Tomato mosaic virus* strain ToMV1-2 contains two independent single resistance-breaking domains. *Archives of Virology*, **152**, 903.

Ueki, S. and Citovsky, V. (2011) To gate, or not to gate: regulatory mechanisms for intercellular protein transport and virus movement in plants. *Molecular plant*, **4**, 782-793.

Waigmann, E., Lucas, W. J., Citovsky, V. and Zambryski, P. (1994) Direct functional assay for *tobacco mosaic virus* cell-to-cell movement protein and identification of a domain involved in increasing plasmodesmal permeability. *Proceedings of the National Academy of Sciences*, **91**, 1433-1437.

Wang, J., Chen, T., Han, M., Qian, L., Li, J., Wu, M. and Hong, Y. (2020) Plant NLR immune receptor Tm-2^2 activation requires NB-ARC domain-mediated self-association of CC domain. *PLoS pathogens*, **16**, e1008475.

Weber, H. and Pfitzner, A.J. (1998) *Tm-2^2* resistance in tomato requires recognition of the carboxy terminus of the movement protein of *Tomato mosaic virus*. *Molecular plant-microbe interactions*, **11**, 498-503.

Weber, H., Schultze, S. and Pfitzner, A.J. (1993) Two amino acid substitutions in the *Tomato mosaic virus* 30-kilodalton movement protein confer the ability to overcome the *Tm-2^2* resistance gene in the tomato. *Journal of Virology*, **67**, 6432-6438.

Weber, H., Ohnesorge, S., Silber, M. V. and Pfitzner, A.J.P. (2004) The *Tomato mosaic virus* 30 kDa movement protein interacts differentially with the resistance genes *Tm-2* and *Tm-2^2*. *Archives of Virology*, **149**, 1499-1514.

Weber, E., Engler, C., Gruetzner, R., Werner, S. and Marillonnet, S. (2011). A modular cloning system for standardized assembly of multigene constructs. *PLoS one*,

6, e16765.

Whitham, S., McCormick, S. and Baker, B. (1996) The *N* gene of tobacco confers resistance to *tobacco mosaic virus* in transgenic tomato. *Proceedings of the National Academy of Sciences*, **93**, 8776-8781.

Yan, Z., Ma, H., Han, S., Geng, C., Tian, Y. and Li, X. (2019) First report of *Tomato brown rugose fruit virus* infecting tomato in China. *Plant Disease*, **103**, 2973-2973.

Zhang, H., Zhao, J., Liu, S., Zhang, D. P. and Liu, Y. (2013) *Tm-2*^{2} confers different resistance responses against tobacco mosaic virus dependent on its expression level. *Molecular Plant*, **6**, 971-974.

Zhu, M., Jiang, L., Bai, B., Zhao, W., Chen, X. *et al.* (2017) The intracellular immune receptor *Sw-5b* confers broad-spectrum resistance to tospoviruses through recognition of a conserved 21-amino acid viral effector epitope. *The Plant Cell*, **29**, 2214-2232.

601 **Figure 1**

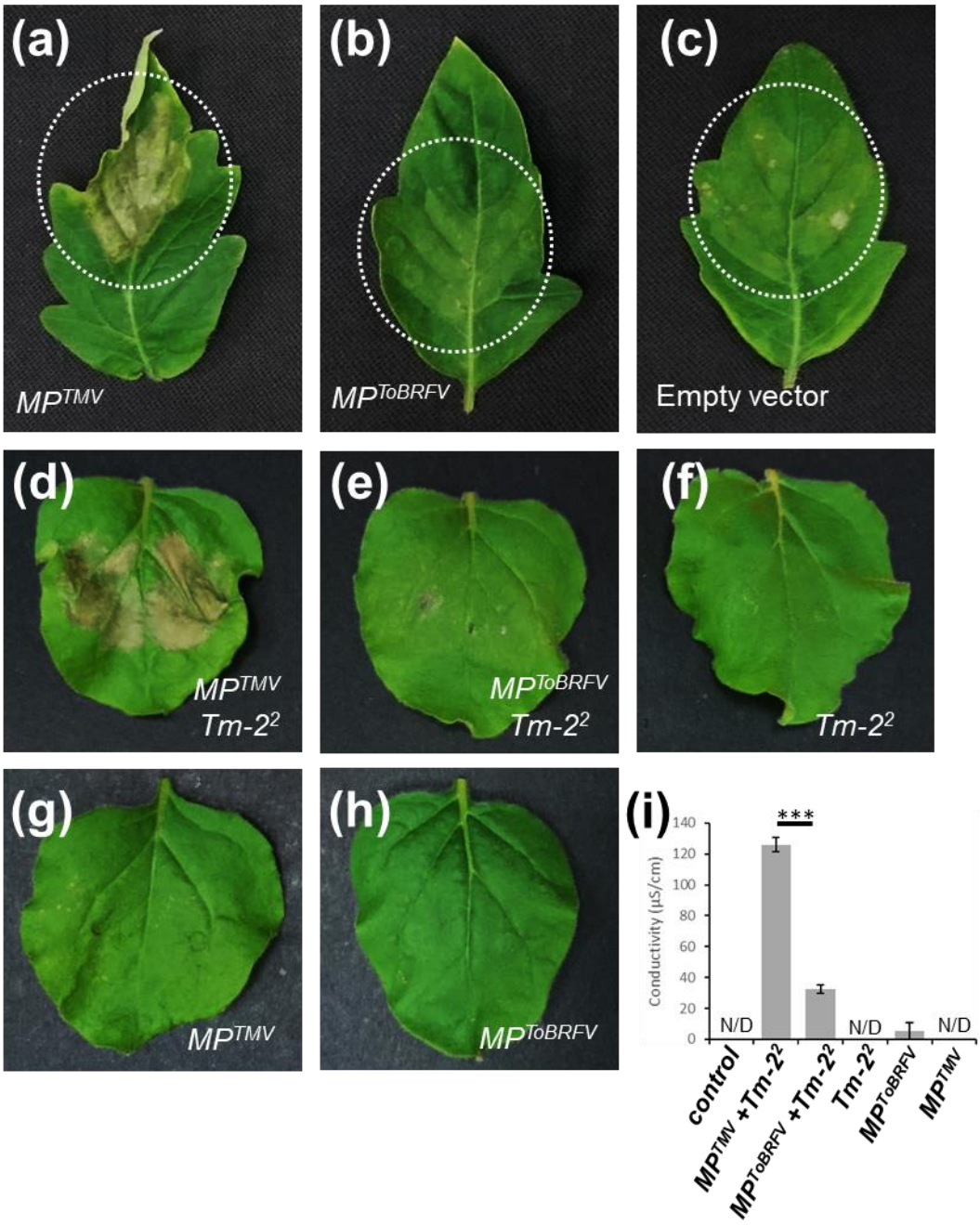

602 **Figure 1. *Tm-2²*-mediated cell death in tomato and *N. benthamiana* in response**
603 **to MP^{TMV} and MP^{ToBRFV}.** (a-c) Transient expression of *MP^{TMV}* (a), *MP^{ToBRFV}* (b) and
and empty vector in tomato cv. Ikram containing the Tm-2^2 resistance gene. (d-h)
604 Transient expression of *MP^{TMV}* with *Tm-2^2* (d), MP^{ToBRFV} with *Tm-2^2* (e), *Tm-2^2* (f),
605 *MP^{TMV}* (g) and MP^{ToBRFV} (h) in *N. benthamiana* leaves. (i) Electrolyte leakage assay
of *N. benthamiana* leaves expressing the various constructs (***P<0.001, student's
606 t-test, $n \geq 4$). N/D = not detected.

607

608 **Figure 2**

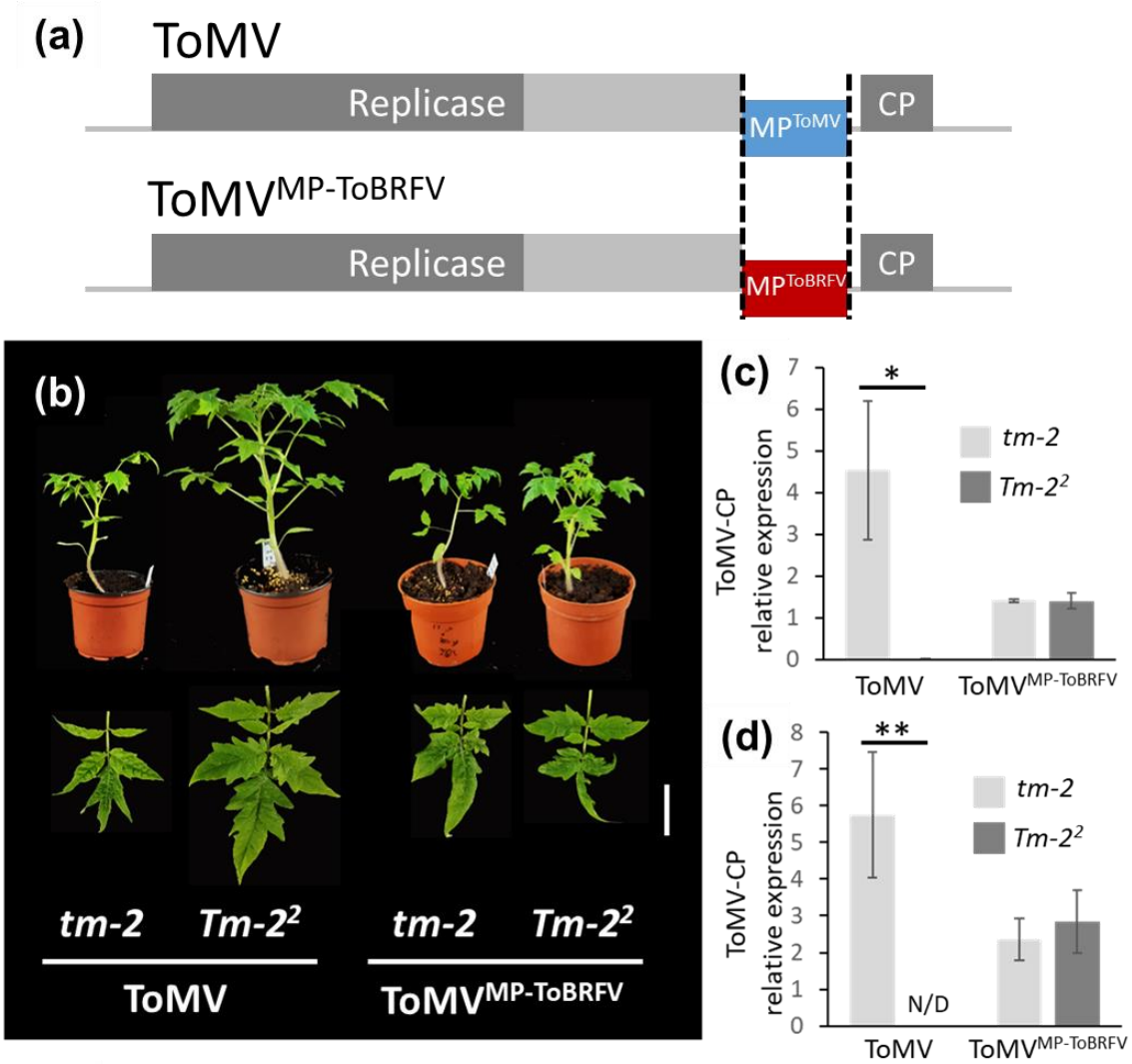

(e)

Virus	Genotype	Symptoms	Infected
ToMV	*tm-2/tm-2*	12/12	12/12
ToMV$^{MP\text{-}ToBRFV}$	*tm-2/tm-2*	11/11	11/11
ToMV	*Tm-2²/Tm-2²*	0/10	0/10
ToMV$^{MP\text{-}ToBRFV}$	*Tm-2²/Tm-2²*	11/11	11/11

609

610 **Figure 2. Replacement of MP^{ToMV} with MP^{ToBRFV} is sufficient to overcome *Tm-2²* resistance in tomato.** (a) Schematic illustration of ToMV and ToMV$^{MP\text{-}ToBRFV}$ viruses.
611 Segmented lines indicate the replacement of MP^{ToMV} (blue) with the MP^{ToBRFV} (red) sequence. (b) Tomato plants (cv. Moneymaker) (upper panel) and leaves (lower panel)
612 homozygous to the *tm-2* or *Tm-2²* allele infected with ToMV and ToMV$^{MP\text{-}ToBRFV}$. (c-d) RT-qPCR analysis for ToMV coat protein (CP) transcripts in locally infected (c) and systemic
613 (d) leaves of *tm-2* and Tm-2² tomato plants infected with ToMV and ToMV$^{MP\text{-}ToBRFV}$. (e) Number of plants showing systemic symptoms of ToMV infection in and results of virus
614 detection by RT-PCR assay (*P<0.05, **P<0.01, student's t-test, $n \geq 4$). N/D = not detected.
615 Scale bar = 2 cm.

Figure 3

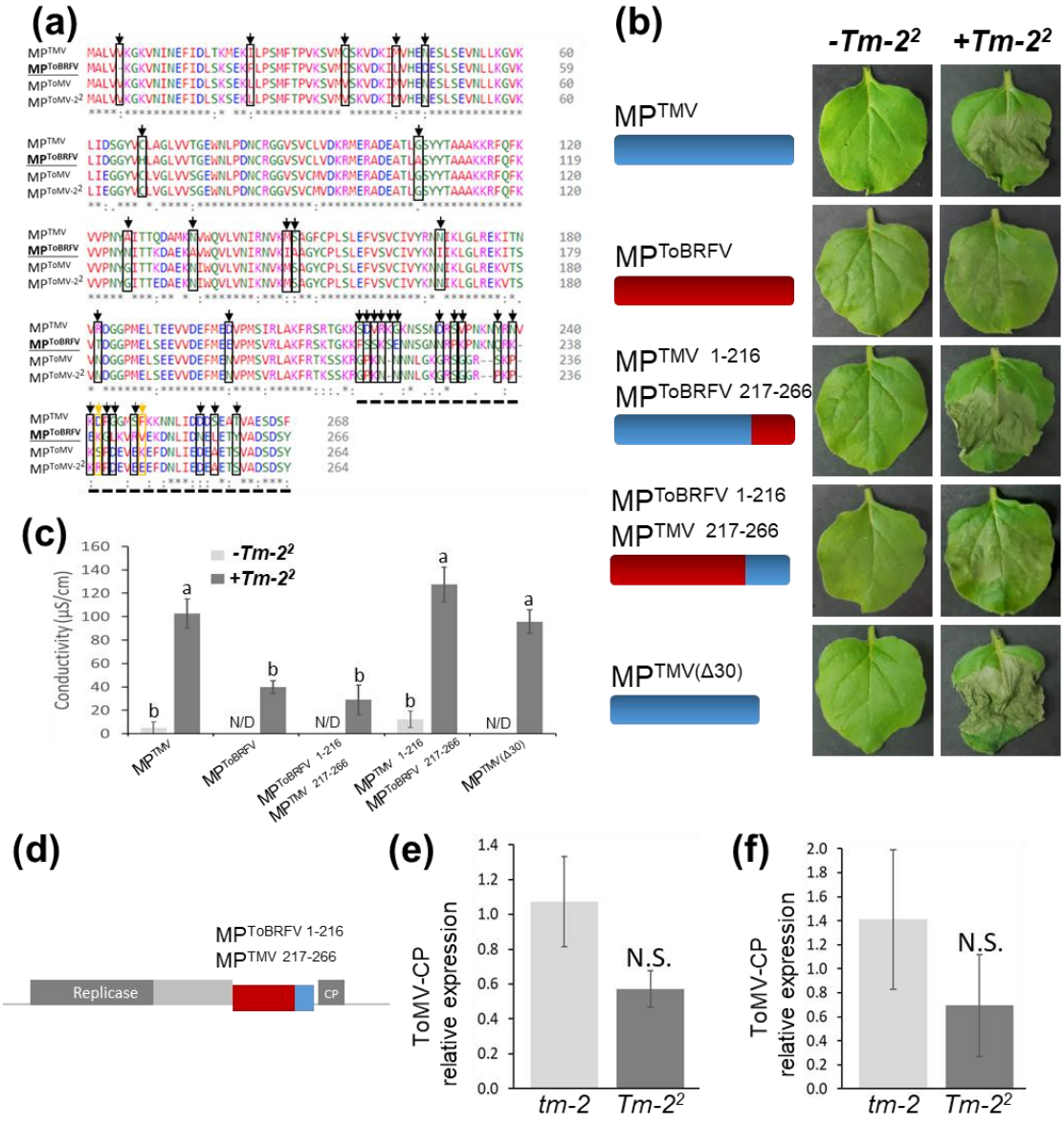

Figure 3. Overcoming *Tm-2*^{2} resistance is not due to the MP^{ToBRFV} C terminus. (a) Amino acid sequence alignment of MP^{ToBRFV} with MP^{TMV}, MP^{ToMV} and the resistance-breaking MP$^{ToMV-22}$. A total of 33 suspected resistance-breaking mutations are highlighted in black. The MP^{ToMV} amino acids Ser238 and Lys244, previously found to be required for Tm-2^2 recognition, are highlighted in yellow. The segmented black line underlies the variable 50 C-terminal amino acids. (b) Transient expression of MP^{TMV}, MP^{ToBRFV}, the hybrids MP$^{ToBRFV\ 1-216}$/MP$^{TMV\ 217-266}$ and MP$^{TMV\ 1-216}$/MP$^{ToBRFV\ 217-266}$ and the truncated MP$^{TMV(\Delta 30)}$ in *N. benthamiana* leaves. Clones were expressed alone (*-Tm-2*^{2}) or co-expressed with *Tm-2*^{2} (*+Tm-2*^{2}). (c) Electrolyte leakage assay of *N. benthamiana* leaves expressing the various constructs. (d) Schematic illustration of the ToMV$^{MP-ToBRFV\ 1-216}$ virus expressing a hybrid movement protein with MP^{ToBRFV} amino acids 1-216 fused to MP^{TMV} amino acids 217-266 (e-f) RT-qPCR analysis for ToMV coat protein (CP) transcripts in infected (e) and systemic (f) leaves of *tm-2* and Tm-2^2 tomato plants infected with ToMV$^{MP-ToBRFV\ 1-216}$. Different letters indicate significant in Tukey's HSD test. ($n \geq 4$). N.S. = not significant.

625

Figure 4

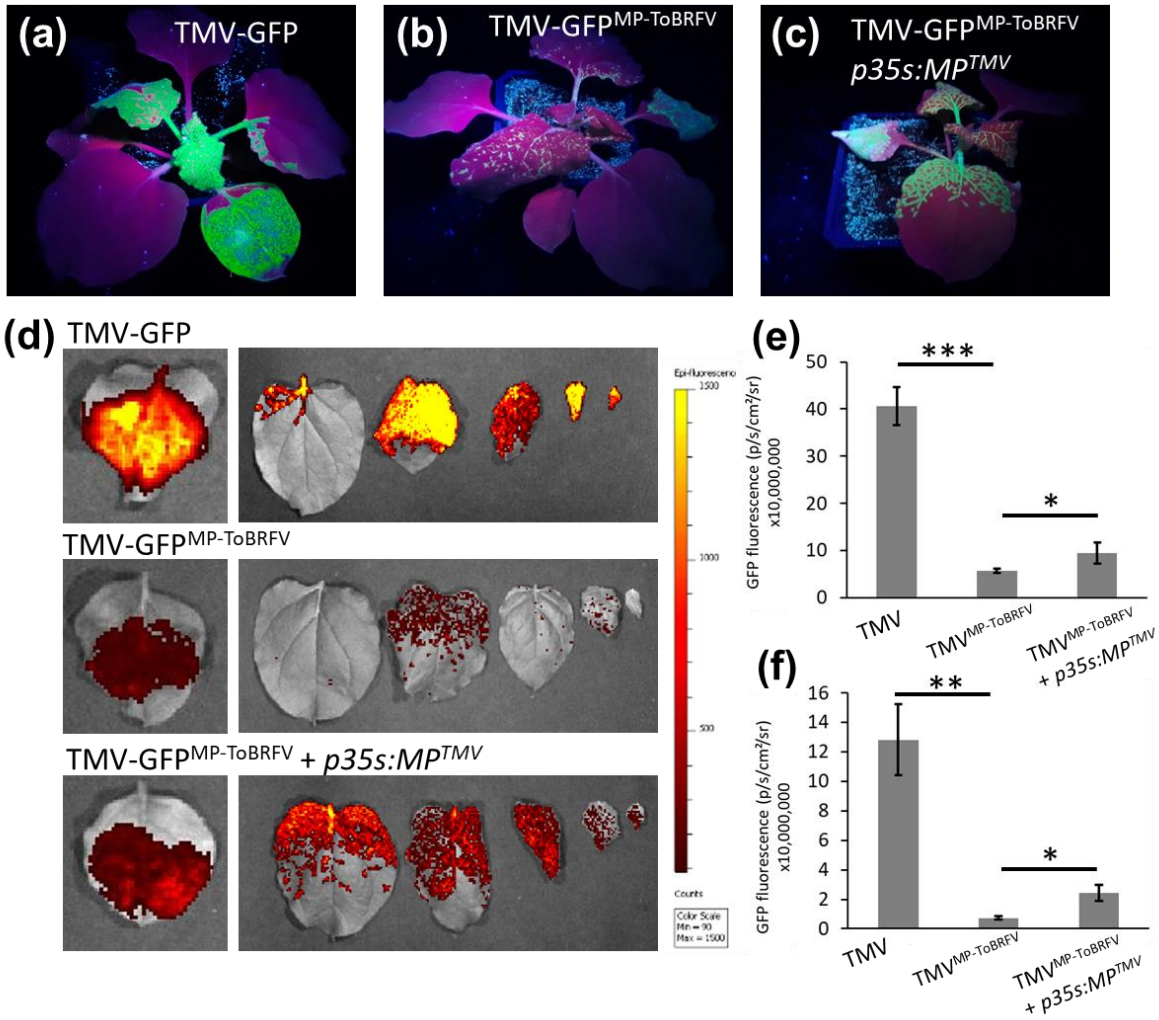

626

627

Figure 4. Replacement of MP^{TMV} with MP^{ToBRFV} causes a reduction in TMV-GFP systemic infection in *N. benthamiana*. (a-c) UV images of *N. benthamiana* plants infected with TMV-GFP (a), TMV-GFP$^{MP\text{-}ToBRFV}$ (b) and TMV-GFP$^{MP\text{-}ToBRFV}$ co-expressed with *p35S:MP^{TMV}* (c). (d) IVIS images of infected (left panel) and systemic leaves 1-4 from the apex (right panel) of infected plants. (d-e) Quantitative analysis of GFP fluorescence in locally infected (e) and systemic (f) leaves of plants expressing TMV-GFP , TMV-GFP$^{MP\text{-}ToBRFV}$ and TMV-GFP$^{MP\text{-}ToBRFV}$ co-expressed with *p35S:MP^{TMV}*. (*P<0.05, **P<0.01, student's t-test, $n \geq 5$).

628

629

630

631

632

633

634

635

636

Figure 5

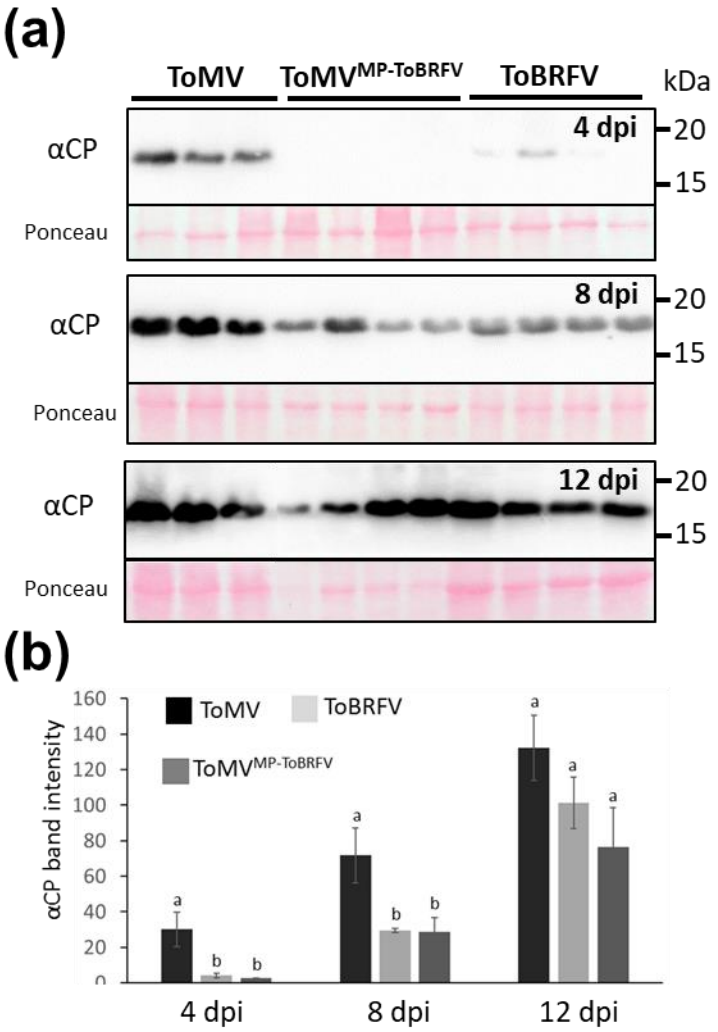

637

638 **Figure 5. Delayed systemic infection by viruses expressing MP^{ToBRFV} in tomato plants.** (a) Western blot analysis of ToMV, ToMV$^{MP\text{-}ToBRFV}$ and
639 ToBRFV coat protein in systemic leaves 4, 8 and 12 days post inoculation (dpi). (b) Quantitative analysis of ToMV, ToMV$^{MP\text{-}ToBRFV}$ and ToBRFV coat
640 proteins in systemic leaves. Note that while ToMV coat proteins are detected in systemic leaves at 4 dpi, ToBRFV and ToMV$^{MP\text{-}ToBRFV}$ coat proteins
641 accumulate later, at 8 dpi. Different letters indicate significantly different values (P <0.05, Tukey's HSD test, $n \geq 4$).

642

643

644

645

646

647

Figure 6

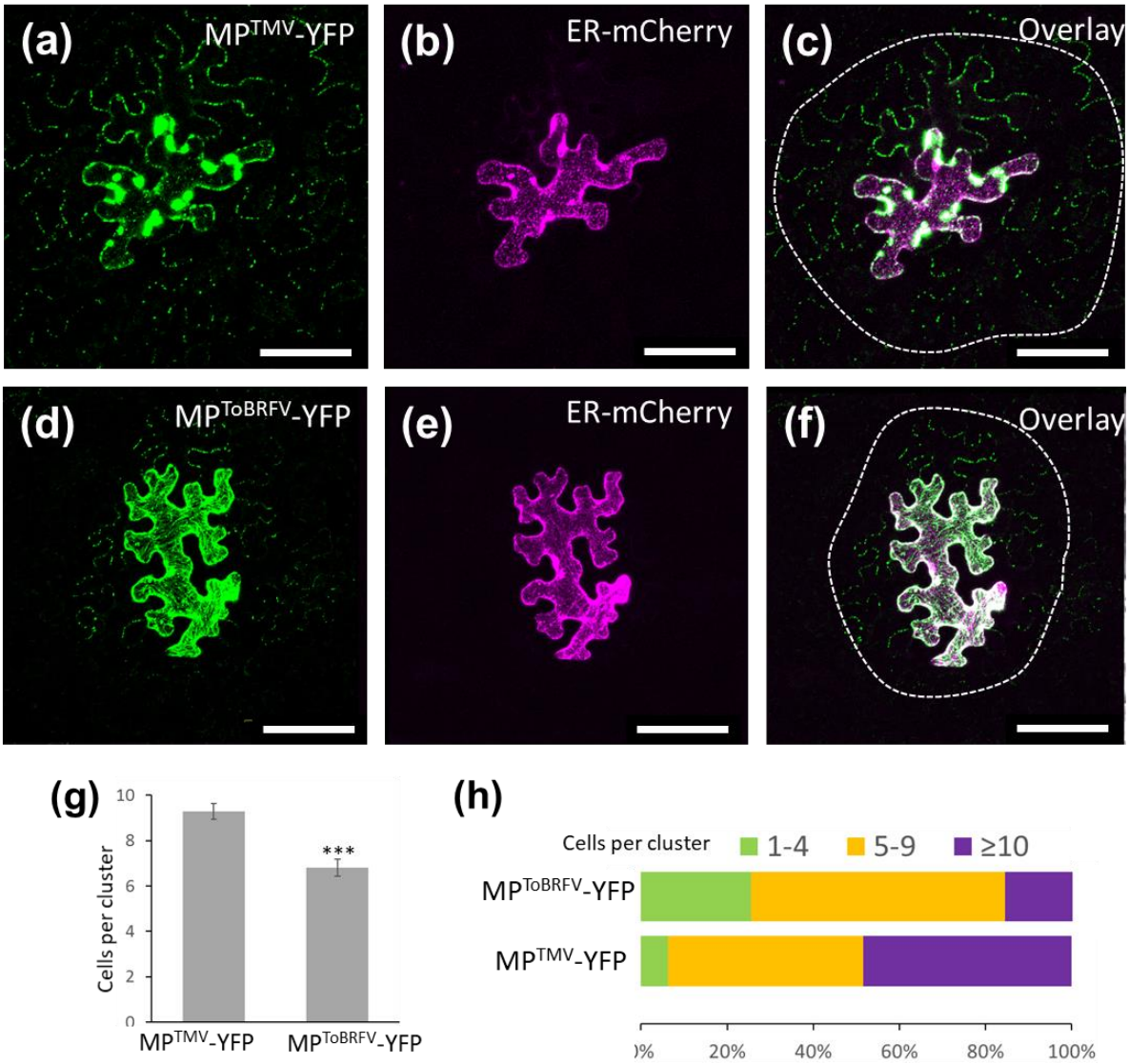

648

649 **Figure 6. Reduced cell-to-cell movement of MP^{ToBRFV} compared to MP^{TMV}.** (a-c)
650 Coexpression of MP^{TMV}-YFP (a) and the non-mobile ER-mCherry (b) in *N. benthamiana*
651 leaf epidermal cells. (c) Overlay of MP^{TMV}-YFP and ER-mCherry. (d-f) Coexpression of
652 MP^{ToBRFV}-YFP (d) and the non-mobile ER-mCherry (e) in *N. benthamiana* leaf epidermal
653 cells. (f) Overlay of MP^{ToBRFV}-YFP and ER-mCherry. Broken white lines circle the
654 cluster of cells to which the MPs moved. (g) Quantitative analysis of the number of cells
per MP^{TMV}-YFP and MP^{ToBRFV}-YFP clusters. (h) Fractionation of MP^{TMV}-YFP and
MP^{ToBRFV}-YFP clusters: 1-4 cells (green), 5-9 cells (yellow) and ≥10 (purple). (***$P <$
0.001, Student's t-test $n \geq 51$). Scale bar = 100 µm.

655

656

657

658 **Figure 7**

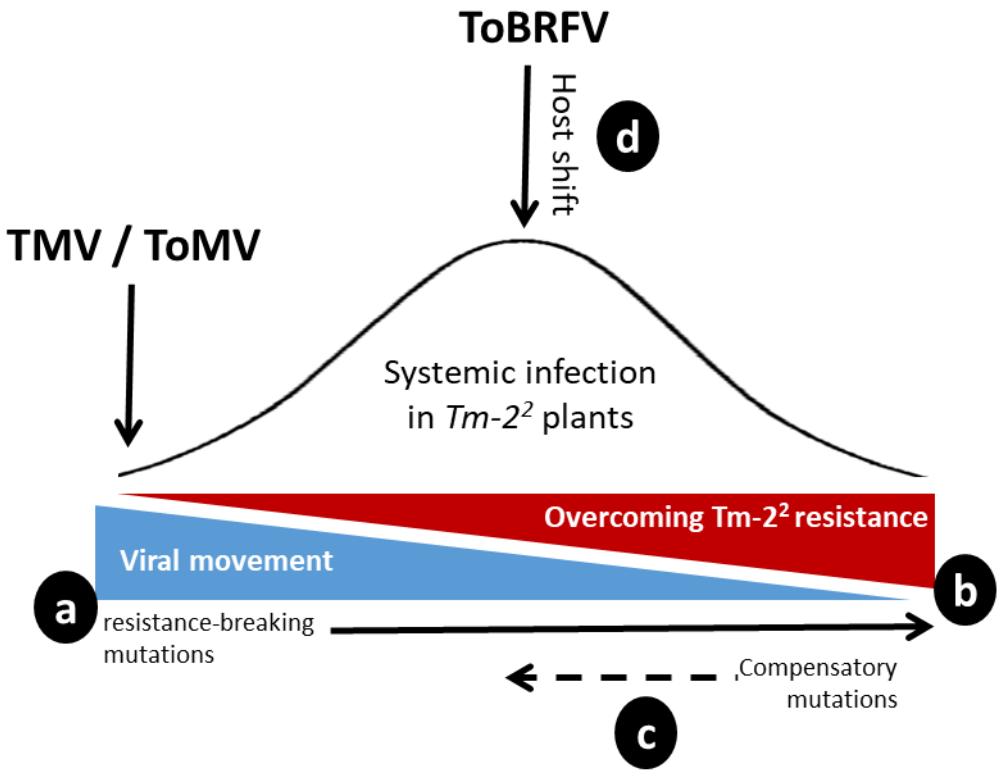

659

660 **Figure 7. Hypothetical model for overcoming *Tm-2²* resistance.** (a) To overcome
661 *Tm-2²* resistance, MP^{TMV} or MP^{ToMV} will develop resistance-breaking mutations,
662 which will likely impair their movement capacity (b). (c) To restore MP function,
663 multiple compensatory mutations would be required. Such processes, which require
multiple rounds of mutation and selection, will be unlikely to occur. (d) ToBRFV,
whose emergence in tomato is likely a result of a host shift, accumulated sufficient
mutations, which enable it to function while not being recognized by Tm-2^2.

664